PROCEEDINGS OF SCIENCE

Heavy-heavy current improvement for calculation of $\bar{B} \to D^{(*)}\ell\bar{\nu}$ semi-leptonic form factors using the Oktay-Kronfeld action

Jon A. Bailey[*], **Jaehoon Leem**[†], **Weonjong Lee**
Lattice Gauge Theory Research Center, CTP, and FPRD,
Department of Physics and Astronomy,
Seoul National University, Seoul 08826, South Korea
E-mail: jonbailey@snu.ac.kr, leemjaehoon@gmail.com, wlee@snu.ac.kr

Yong-Chull Jang
Los Alamos National Laboratory,
Theoretical Division T-2, MS B283,
Los Alamos, New Mexico 87545, USA
E-mail: integration.field@gmail.com

SWME Collaboration

Lattice calculations of the form factors for $\bar{B} \to D^{(*)}\ell\bar{\nu}$ decays can be used to extract the CKM matrix element $|V_{cb}|$. The Oktay-Kronfeld action is a highly improved version of the Fermilab action, which systematically reduces heavy quark discretization effects through $\mathcal{O}(\lambda^3)$ in HQET power counting, for heavy-light meson quantities. To calculate $\bar{B} \to D^{(*)}\ell\bar{\nu}$ semi-leptonic form factors using Oktay-Kronfeld heavy quarks, we need to improve the heavy quark currents to the same level. We report our progress in calculating the improvement coefficients for currents composed of bottom and charm quarks. Our results presented in this paper are preliminary.

34th Annual International Symposium on Lattice Field Theory
24-30 July 2016
University of Southampton, UK

[*]Speaker.
[†]Speaker.

© Copyright owned by the author(s) under the terms of the Creative Commons Attribution-NonCommercial-NoDerivatives 4.0 International License (CC BY-NC-ND 4.0).

arXiv:1612.09081v1 [hep-lat] 29 Dec 2016

1. Introduction

Precision tests of the Standard Model (SM) in the flavor sector are crucial to the search for new physics. The SM requires unitarity of the Cabibbo-Kobayashi-Maskawa (CKM) quark mixing matrix, and the CKM matrix element $|V_{cb}|$ plays a central role because it normalizes the unitarity triangle. By calculating $\bar{B} \to D^{(*)}\ell\bar{\nu}$ decay form factors on the lattice and combining them with experimental results for the branching fractions, one can determine $|V_{cb}|$. The decay rates for these processes are given by

$$\frac{d\Gamma}{dw}(\bar{B} \to D\ell\bar{\nu}) = \frac{G_F^2|V_{cb}|^2 m_B^5}{48\pi^3}(w^2-1)^{3/2} r^3 (1+r)^2 |\eta_{\rm EW}|^2 |\mathscr{F}_D(w)|^2, \tag{1.1}$$

$$\frac{d\Gamma}{dw}(\bar{B} \to D^*\ell\bar{\nu}) = \frac{G_F^2|V_{cb}|^2 m_B^5}{48\pi^3}(w^2-1)^{1/2} r^{*3} (1-r^*)^2 \times \left[1 + \frac{4w}{w+1}\frac{1-2wr^*+r^{*2}}{(1-r^*)^2}\right] |\eta_{\rm EW}|^2 |\mathscr{F}_{D^*}(w)|^2, \tag{1.2}$$

where $w = v_B \cdot v_{D^{(*)}}$ is the recoil parameter, $r^{(*)} = m_{D^{(*)}}/m_B$ are the ratios of the daughter to parent meson masses, $\eta_{\rm EW}$ incorporates higher order electroweak corrections, and $\mathscr{F}_{D^{(*)}}(w)$ are the hadronic form factors.

The most precise results for $|V_{cb}||\eta_{\rm EW}||\mathscr{F}_{D^{(*)}}(1)|$ from experimental measurements by BABAR [1, 2, 3] and Belle [4] have uncertainties of a few percent. Recently the Fermilab-MILC Collaboration extracted $|V_{cb}|$ *via* lattice calculations of the form factors for $\bar{B} \to D^*\ell\bar{\nu}$ at zero recoil [5] and $\bar{B} \to D\ell\bar{\nu}$ at nonzero recoil [6, 7]. The results have $2-5\%$ total uncertainties and are consistent with one another and the determination of the $\bar{B} \to D\ell\bar{\nu}$ form factors by the HPQCD Collaboration [8]. If we can reduce the discretization errors in lattice calculations of the form factors, then we can determine $|V_{cb}|$ to higher precision.

The Fermilab-MILC Collaboration used the Fermilab action for the b and c quarks. The Fermilab improvement program controls lattice cutoff effects at any quark mass [9]. To reduce heavy-quark discretization errors, Oktay and Kronfeld extended the improvement of the Fermilab (clover) action to higher order, including mass dimension 6 and 7 operators, or through third order in HQET power counting. Tests of the tree-level matched Oktay-Kronfeld (OK) action yield promising results [10, 11, 12]. For systematic improvement of form factor calculations, the flavor-changing currents must be improved to the same level. The authors of Ref. [9] defined improved currents in terms of an improved heavy quark field. We begin our construction of improved currents by extending the improved field to include operators corresponding to mass dimensions 5 and 6.

In Ref. [13] we considered the improvement of two-quark matrix elements of the flavor-changing currents. We showed that these matrix elements can be matched through third order in expansions of the heavy quark momenta and wrote down results for four of the 11 improvement parameters entering the improved heavy quark fields. In Sec. 2 we further discuss current improvement and the improved heavy quark field. We present details of the matching process and results for the remaining seven improvement parameters in Sec. 3. Section 4 contains a status summary and outstanding issues.

2. Current improvement

The mass-dependent renormalization program begins with the observation that improved Wilson actions can be tuned to the renormalized trajectory by lifting the constraint of time-space axis interchange symmetry, including only irrelevant operators that do not lead to modifications of the Wilson time derivative. The resulting class of actions are constructed to approach the continuum limit for any quark mass, including quark masses large in lattice units.

Consequently, the improvement parameters are functions of the quark masses, *i.e.*, mass-dependent [9]. In this context one may use suitable generalizations of the Symanzik action, HQET, or NRQCD as effective continuum field theories to describe the physics of the resulting lattice theory, including cutoff effects [14, 15, 16]. These descriptions are useful for designing improved actions and currents, assessing improvement, and quantifying remaining (systematic) discretization effects [15, 16, 17, 18].

The Oktay-Kronfeld action was designed to reduce charm quark discretization errors to less than about 1%; bottom quark discretization errors are even smaller [15]. Improvement of the heavy quark currents proceeds in the same way, in principle: All operators with the quantum numbers of the desired currents are included, through a given order in the power counting [9],

$$J_{\rm QCD} = Z_J(am_q, g^2) \left[J_0 + \sum_i C_i(am_q, g^2) J_i \right] . \tag{2.1}$$

The coefficients C_i of the improvement operators J_i, together with the renormalization factors Z_J, are fixed by matching matrix elements to their continuum values [9]. The matching can be carried out using the power counting of the effective continuum field theory to systematize improvement, and for arbitrary fermion masses [9, 17, 18].

In practice, for improvement through first order in HQET, introducing an improved heavy quark field suffices. The improved current can be written

$$J_\Gamma = \bar{\Psi}_{Ic} \Gamma \Psi_{Ib} \,, \tag{2.2}$$

where Γ indicates the Dirac structure, and Ψ_{If} is the improved heavy quark field for flavor $f = c, b$,

$$\Psi_{If}(x) = e^{M_{1f}/2} (1 + d_{1f} \boldsymbol{\gamma} \cdot \boldsymbol{D}) \psi_f(x) \,, \tag{2.3}$$

where M_{1f} is the tree-level rest mass of f quarks, d_{1f} is the improvement parameter, which depends on this rest mass, $\boldsymbol{D}$ is the lattice (symmetric) covariant derivative, and ψ_f is the heavy quark field appearing in the mass form of the action. (Unless explicitly indicated, we set the lattice spacing $a = 1$.) The results for the improvement parameters d_{1f} at tree-level were first written down in Ref. [9]; these results were obtained by tree-level matching of two-quark matrix elements of the flavor-changing currents. The authors of Refs. [17, 18] then showed that the current defined by Eqs. (2.2) and (2.3) is improved through first order in HQET power counting.

For improvement of two-quark matrix elements through third order in the momenta of the heavy quarks, an improved field again suffices, with the ansatz [13]

$$\Psi_I(x) = e^{M_1/2} \left[1 + d_1 \boldsymbol{\gamma} \cdot \boldsymbol{D} + \frac{1}{2} d_2 \Delta^{(3)} + \frac{1}{2} i d_B \boldsymbol{\Sigma} \cdot \boldsymbol{B} + \frac{1}{2} d_E \boldsymbol{\alpha} \cdot \boldsymbol{E} \right.$$

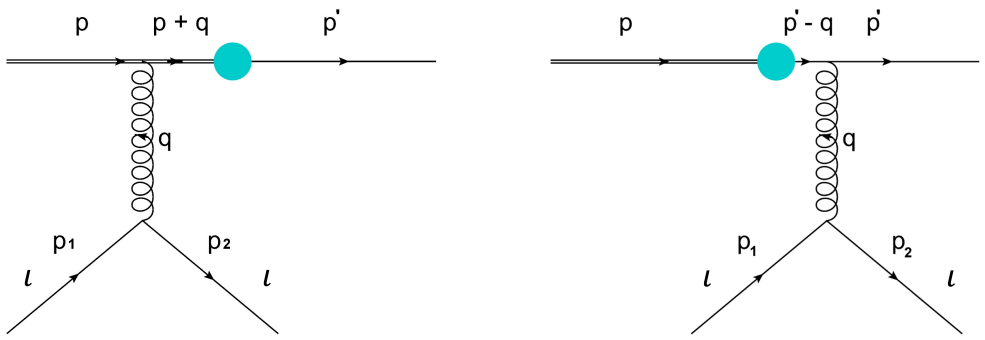

(a) (b)

Figure 1: Tree-level, continuum diagrams for the four-quark matrix element. The colored circle represents the flavor-changing current. (a) The diagram with gluon exchange at the heavy-quark line. (b) The diagram with gluon exchange at the light-quark line.

$$
\begin{aligned}
&+ d_{r_E}\{\boldsymbol{\gamma}\cdot\boldsymbol{D},\boldsymbol{\alpha}\cdot\boldsymbol{E}\} + d_{z_E}\gamma_4(\boldsymbol{D}\cdot\boldsymbol{E} - \boldsymbol{E}\cdot\boldsymbol{D}) \\
&+ \frac{1}{6}d_3\gamma_i D_i\Delta_i + \frac{1}{2}d_4\{\boldsymbol{\gamma}\cdot\boldsymbol{D},\Delta^{(3)}\} + d_5\{\boldsymbol{\gamma}\cdot\boldsymbol{D}, i\boldsymbol{\Sigma}\cdot\boldsymbol{B}\} \\
&+ d_{EE}\{\gamma_4 D_4,\boldsymbol{\alpha}\cdot\boldsymbol{E}\} + d_{z_3}\boldsymbol{\gamma}\cdot(\boldsymbol{D}\times\boldsymbol{B} + \boldsymbol{B}\times\boldsymbol{D})\Big]\psi(x)\,. \qquad (2.4)
\end{aligned}
$$

Matching two-quark matrix elements at tree-level yields results for the parameters d_1, d_2, d_3, and d_4 [13]. The remaining seven improvement parameters in this ansatz do not enter tree-level calculations of the two-quark matrix elements and so are not determined by tree-level matching calculations of these matrix elements. To determine these parameters we match four-quark matrix elements of the currents, at tree-level, as described below.

3. Matching

To obtain improvement parameters through third order in HQET, we consider the following four-quark matrix element of flavor-changing currents,

$$\langle \ell(\eta_2,p_2)u(\eta',p')|\bar{\psi}_u\Gamma\Psi_b|b(\eta,p)\ell(\eta_1,p_1)\rangle_{\rm lat}\,, \qquad (3.1)$$

where ℓ represents a light spectator quark, and u and b indicate an up quark and a bottom quark, respectively. We consider the transition to the light (up) quark rather than to the heavy (charm) quark to simplify the calculation; diagrams with improvement terms on the daughter quark line are eliminated. Accordingly, the field ψ_u appears in Eq. (3.1).

The corresponding continuum, tree-level diagrams are given in Figs. 1(a) and 1(b). The gluon exchange may occur at the external line of the b-quark or the u-quark. In the case of gluon exchange at the u-quark line, however, the matching condition from the diagram is equivalent to that from the two-quark matrix element mentioned above.

Therefore, the part we need to consider is the one-gluon exchange vertex at the b-quark line. The corresponding lattice diagrams are given in Figs. 2(a) and 2(b). In addition to one-gluon

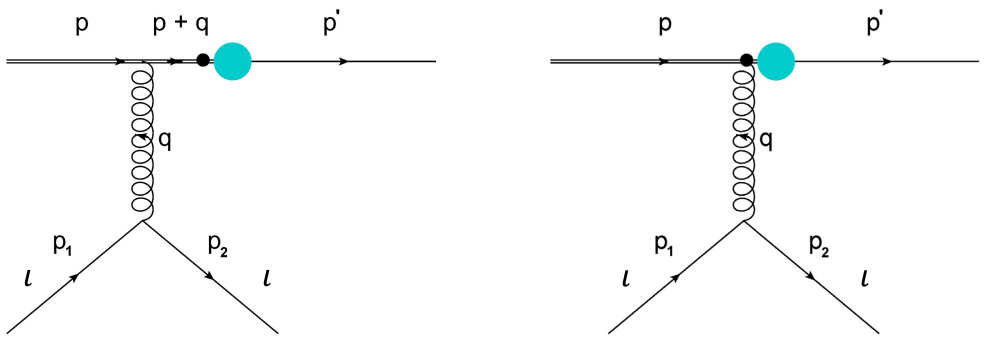

(a) (b)

Figure 2: Tree-level, lattice diagrams with gluon exchange at the heavy-quark line. The dots represent (a) the zero-gluon vertex and (b) the one-gluon vertex from the improved quark field, respectively.

exchange from the action vertices [Fig. 2(a)], one-gluon exchange occurs from vertices of the improvement terms in the quark field [Fig. 2(b)]; these vertices are represented by the dots in Figs. 2(a) and 2(b). The corresponding sub-diagrams in the continuum and lattice theories are

$$\mathscr{M}_\mu = (-gt^a) S_b(p+q)\gamma_\mu \sqrt{\frac{m_b}{E_b}} u_b(\eta,p) = (-gt^a)\frac{m_b - i\gamma\cdot(p+q)}{m_b^2+(p+q)^2}\gamma_\mu \sqrt{\frac{m_b}{E_b}} u_b(\eta,p), \tag{3.2}$$

$$\mathscr{M}^{\rm lat}_\mu = (-gt^a) n_\mu(q)\left[R_b^{(0)}(p+q) S_b^{\rm lat}(p+q)\Lambda_\mu(p+q,p) + R^{(1)}_{b,\mu}(p+q,p)\right]\mathscr{N}_b(p) u_b^{\rm lat}(\eta,p), \tag{3.3}$$

where q is the momentum of the virtual gluon; p is the external b-quark momentum; the factor $n_\mu(q) = 2\sin\left(\frac{1}{2}q_\mu\right)/q_\mu = 1 - \frac{1}{24}q_\mu^2 + \cdots$ is the lattice wave-function factor for the gluon line; $S_b(p+q)$ and $S_b^{\rm lat}(p+q)$ are the continuum and lattice b-quark propagators, respectively; $\mathscr{N}_b(p)u_b^{\rm lat}(\eta,p)$ is the normalized lattice spinor from the OK action, which corresponds to the normalized spinor $\sqrt{\frac{m_b}{E_b}}u_b(\eta,p)$ in the continuum; Λ_μ denotes the one-gluon exchange vertex from the OK action; $R_b^{(0)}$ denotes zero-gluon vertices from the improvement terms in the heavy quark field; and $R^{(1)}_{b,\mu}$ denotes one-gluon vertices from the improvement terms in the heavy quark field.

The improvement parameters d_1, d_2, d_3, and d_4 enter *via* the zero-gluon exchange vertices $R_b^{(0)}$,

$$\begin{aligned} R_b^{(0)}(p+q) = e^{M_1/2}\Bigg[& 1 + id_1\sum_j \gamma_j \sin(p_j+q_j) - 2d_2\sum_j \sin^2\frac{1}{2}(p_j+q_j) \\ & - \frac{2}{3}id_3\sum_j \gamma_j\sin(p_j+q_j)\sin^2\frac{1}{2}(p_j+q_j) - 4id_4\sum_{j,k}\gamma_j\sin(p_j+q_j)\sin\frac{1}{2}(p_k+q_k)\Bigg]. \end{aligned} \tag{3.4}$$

The remaining seven improvement parameters enter *via* the one-gluon exchange vertices $R^{(1)}_{b,\mu}$. The temporal ($\mu = 4$) component is

$$R^{(1)}_{b,4}(p+q,p) = e^{M_1/2}\cos\frac{1}{2}q_4\gamma_4\left[\frac{i}{2}d_E\zeta\sum_j\gamma_j\sin q_j - d_{EE}\gamma_4\sum_j\gamma_j\sin q_j\left[\sin(p_4+q_4)-\sin(p_4)\right]\right.$$

$$+(d_{r_E}-d_{z_E})\sum_j \sin q_j\big[\sin(p_j+q_j)-\sin p_j\big]-id_{r_E}\sum_{j,l,m}\varepsilon_{jlm}\Sigma_j\sin q_l\big[\sin(p_m+q_m)+\sin p_m\big]\Bigg], \tag{3.5}$$

while the spatial ($\mu = i$) components are

$$\begin{aligned}
R^{(1)}_{b,i}(p+q,p) = e^{M_1/2}\Bigg[& -d_1\gamma_i\cos(p_i+\frac{1}{2}q_i)-id_2\sin(p_i+\frac{1}{2}q_i)-\frac{1}{2}d_B\sum_{r,m}\varepsilon_{irm}\Sigma_m\sin q_r\cos\frac{1}{2}q_i \\
& -\frac{i}{2}d_E\gamma_4\gamma_i\cos\frac{1}{2}q_i\sin q_4+d_{r_E}\sum_{r,m}i\varepsilon_{irm}\Sigma_m\gamma_4\sin q_4\big[\sin(p_r+q_r)+\sin p_r\big]\cos\frac{1}{2}q_i \\
& -(d_{r_E}-d_{z_E})\gamma_4\sin q_4\big[\sin(p_i+q_i)-\sin p_i\big]\cos\frac{1}{2}q_i+d_{EE}\gamma_i\sin q_4\big[\sin(p_4+q_4)-\sin p_4\big]\cos\frac{1}{2}q_i \\
& +\frac{1}{2}d_4\Bigg[\gamma_i\cos(p_i+\frac{1}{2}q_i)\sum_j 4\big[\sin^2\frac{1}{2}(p_j+q_j)+\sin^2\frac{1}{2}p_j\big]+2\sin(p_i+\frac{1}{2}q_i)\sum_j\gamma_j\big[\sin(p_j+q_j)+\sin p_j\big]\Bigg] \\
& +\frac{1}{12}d_3\gamma_i\Bigg[4\cos(p_i+\frac{1}{2}q_i)\big[\sin^2\frac{1}{2}(p_i+q_i)+\sin^2\frac{1}{2}p_i\big]+2\sin(p_i+\frac{1}{2}q_i)\big[\sin(p_i+q_i)+\sin p_i\big]\Bigg] \\
& +(d_5-d_{z_3})\cos\frac{1}{2}q_i\Big[-\sum_j\gamma_j\sin q_j\big[\sin(p_i+q_i)-\sin p_i\big]+\gamma_i\sum_j\sin q_j\big[\sin(p_j+q_j)-\sin q_j\big]\Big] \\
& +d_5\cos\frac{1}{2}q_i\gamma_4\gamma_5\sum_{r,m}\varepsilon_{irm}\sin q_r\big[\sin(p_m+q_m)+\sin p_m\big]\Bigg].
\end{aligned} \tag{3.6}$$

In these expressions the momentum p of the heavy quark is on shell, $p_4 = iE_b = i\left[M_1+\dfrac{\boldsymbol{p}^2}{2M_2}+\cdots\right]$.

Assuming the spatial momentum $\boldsymbol{p}$ of the external b-quark and the gluon momentum transfer q are much smaller than the b-quark mass m_b and the inverse of the lattice spacing $1/a$, we expand $\mathscr{M}^{\rm lat}_\mu$ and $\mathscr{M}_\mu$ in $\boldsymbol{p}a$, qa, $\boldsymbol{p}/m_b$, and q/m_b. We then equate the coefficients of the expansions of $\mathscr{M}^{\rm lat}_\mu$ and $\mathscr{M}_\mu$ at each order in $\boldsymbol{p}$ and q. The resulting equations constrain the improvement parameters d_i from the improvement vertices $R^{(0)}_b$ and $R^{(1)}_{b,\mu}$. Each improvement parameter d_i may appear in more than one constraint equation. The parameters d_E, d_{r_E}, d_{z_E}, and d_{EE} appear in both the temporal ($\mu = 4$) and spatial ($\mu = i$) components of the one-gluon exchange vertex $R^{(1)}_{b,\mu}$. The constraint equations for $\mu = 4$ and $\mu = i$ must be consistent.

For example, consider the constraint equation for the improvement parameter d_{EE} from the $\mu = 4$ components of the amplitudes. The parameter d_{EE} enters *via* one of the terms in the one-gluon exchange vertex $R^{(1)}_{b,4}$. Expanding this term in $\boldsymbol{p}$ and q, we obtain

$$-d_{EE}\cos(\frac{1}{2}q_4)\sum_j\gamma_j\sin q_j\big[\sin(p_4+q_4)-\sin(p_4)\big] = -d_{EE}\cosh M_1\boldsymbol{\gamma}\cdot\boldsymbol{q}q_4+\cdots. \tag{3.7}$$

Then the lowest order constraint equation on d_{EE} from Eqs. (3.2) and (3.3) is

$$\left[\frac{\zeta e^{-M_1}\cosh M_1}{8\sinh^3 M_1}+\frac{\zeta c_E e^{-M_1}}{8\sinh^2 M_1}+\frac{c_{EE}}{2\tanh M_1}-d_{EE}\cosh M_1\right]\boldsymbol{\gamma}\cdot\boldsymbol{q}q_4u(\eta,0) = \frac{\boldsymbol{\gamma}\cdot\boldsymbol{q}q_4}{8m_b^3}u(\eta,0), \tag{3.8}$$

where we gather all linearly dependent terms at leading order of the Taylor expansions and equate them.

For the case $\mu = i$, we obtain the lowest order constraint equation for d_{EE} in the same manner,

$$\left[\frac{\zeta e^{-M_1}\cosh M_1}{8\sinh^3 M_1}+\frac{\zeta c_E e^{-M_1}}{8\sinh^2 M_1}+\frac{c_{EE}}{2\tanh M_1}-d_{EE}\cosh M_1\right]q_4^2\gamma_i u(\eta,0)=\frac{1}{8m_b^3}q_4^2\gamma_i u(\eta,0)\,, \quad (3.9)$$

which yields exactly the same constraint as Eq. (3.8).

We have obtained constraint equations on all the improvement parameters in the ansatz of Eq. (2.4). We have checked that all the constraint equations are consistent through first order in $\boldsymbol{p}$. We expect $\mathscr{M}_\mu^{\rm lat}$ and $\mathscr{M}_\mu$ to match through $\mathscr{O}(\boldsymbol{p}^3)$, given the values we obtain for the 11 improvement parameters in Eq. (2.4). Our results for $d_1 - d_4$ are consistent with those reported in Ref. [13], while for the parameters d_B, d_E, d_{EE}, d_{r_E}, d_{z_E}, d_{z_3}, and d_5, we obtain

$$d_B = d_1^2 - \frac{r_s\zeta}{2(1+m_0)}, \quad (3.10)$$

$$d_E = \frac{1}{2m_b^2}-\frac{\zeta(1+m_0)(m_0^2+2m_0+2)}{[m_0(2+m_0)]^2}+\frac{\zeta(1+m_0)(1-c_E)}{m_0(2+m_0)}, \quad (3.11)$$

$$\begin{aligned} d_{r_E} = {} & -\frac{1}{8m_b^3}+\frac{r_s\zeta}{24(1+m_0)}+\frac{\zeta c_{EE}(2+2m_0+m_0^2)}{2m_0(1+m_0)(2+m_0)}+\frac{\zeta^2 c_E(2+2m_0+m_0^2)}{[2m_0(2+m_0)]^2} \\ & +\frac{\zeta^2(12+24m_0+16m_0^2+4m_0^3+m_0^4)}{12m_0^3(2+m_0)^3}-d_1\frac{\zeta(1+m_0)[2+m_0(2+m_0)c_E]}{2m_0^2(2+m_0)^2}, \end{aligned} \quad (3.12)$$

$$\begin{aligned} d_{EE} = {} & \frac{1+m_0}{(m_0^2+2m_0+2)}\Big[-\frac{1}{4m_b^3}+\frac{\zeta(1+m_0)(m_0^2+2m_0+2)}{[m_0(2+m_0)]^3} \\ & +\frac{\zeta c_E(1+m_0)}{[m_0(2+m_0)]^2}+\frac{(2+2m_0+m_0^2)c_{EE}}{m_0(2+m_0)}\Big], \end{aligned} \quad (3.13)$$

$$\begin{aligned} d_5 = {} & -\frac{1}{16m_b^3}+\frac{\zeta c_B[(1+m_0)(4+6m_0+3m_0^2)\zeta - m_0^2(2+m_0)^2 d_1]}{8(1+m_0)[m_0(2+m_0)]^2}+\frac{c_3(1+m_0)}{m_0(2+m_0)} \\ & +\frac{\zeta^2 c_E[d_1 m_0(2+m_0)-\zeta(1+m_0)]}{4[m_0(2+m_0)]^2}+\frac{-\zeta^2 d_1+\zeta(1+m_0)\left[\frac{(2+2m_0+m_0^2)\zeta^2}{[m_0(2+m_0)]^2}+d_B\right]}{4m_0(2+m_0)}, \end{aligned} \quad (3.14)$$

$$d_{z_E} = d_{z_3} = 0. \quad (3.15)$$

4. Status and outstanding issues

Results for the improvement parameters appearing in our ansatz for the improved heavy quark field are contained in Eqs. (3.10)-(3.15). These results are obtained by matching the two- and four-quark flavor-changing current matrix elements at zeroth and first order in expansions in the momenta of the heavy quarks. To simplify the matching of the four-quark matrix elements, we consider the $b \to u$ (heavy to light) transition instead of the $b \to c$ (heavy to heavy) transition, expand in the momentum transfer along the gluon line, and match through second order in the momentum transfer.

To cross-check the results in Eqs. (3.10)-(3.15), we have performed two independent sets of matching calculations. From the matching conditions for the two- and four-quark matrix elements,

we find multiple independent constraints on the 11 improvement parameters. From these constraints we also verify that the improvement parameters in Eqs. (3.10)-(3.15) are consistent with the results for the improvement parameters in the OK action [15].

However, several issues remain. To summarize:

1. Several of our results for the improvement parameters diverge as the bare mass $m_0 \to 0$. Since we expect a smooth connection with the improved currents of a relativistic lattice theory in this limit, this divergent behavior appears suspicious, at least at first glance. For example, consider the parameter d_4 [13].

$$d_4 = -\frac{d_1}{8M_X^2} + \frac{d_2\zeta}{4\sinh M_1} + \frac{3}{16}\left(\frac{1}{M_Y^3} - \frac{1}{m_b^3}\right), \tag{4.1}$$

where

$$d_1 = \frac{\zeta}{2\sinh M_1} - \frac{1}{2m_b}, \tag{4.2}$$

$$d_2 = d_1^2 - \frac{r_s\zeta}{2e^{M_1}}, \tag{4.3}$$

$$\frac{1}{M_X^2} = \frac{\zeta^2}{\sinh^2 M_1} + \frac{2r_s\zeta}{e^{M_1}}, \tag{4.4}$$

$$\frac{1}{M_Y^3} = \frac{8}{3\sinh M_1}\left\{2c_2 + \frac{1}{4}e^{-M_1}\left[\zeta^2 r_s(2\coth M_1 + 1) + \frac{\zeta^3}{\sinh M_1}\left(\frac{e^{-M_1}}{2\sinh M_1} - 1\right)\right] + \frac{\zeta^3}{4\sinh^2 M_1}\right\}. \tag{4.5}$$

The relationships among the rest mass, kinetic mass, and bare mass of the quark are

$$aM_1 = \log(1+am_0) = am_0 - \frac{1}{2}(am_0)^2 + \frac{1}{3}(am_0)^3 + \ldots \tag{4.6}$$

$$aM_2 = \frac{(1+am_0)((1+am_0)^2-1)}{\zeta[-r_s + r_s(1+am_0)^2 + 2\zeta(1+am_0)]} = am_0 - \frac{1}{2}(am_0)^2 + (am_0)^3 + \ldots \tag{4.7}$$

where we set $\zeta = r_s = 1$. Since $m_b = M_2$, we obtain, in the limit $am_0 \to 0$,

$$d_1 = \frac{1}{4}(am_0) - \frac{3}{8}(am_0)^2 + \frac{7}{16}(am_0)^3 + \ldots \tag{4.8}$$

$$d_2 = -\frac{1}{2} + \frac{1}{2}(am_0) - \frac{7}{16}(am_0)^2 + \ldots \tag{4.9}$$

$$d_4 = \frac{1}{8}\frac{1}{am_0} - \frac{3}{32} - \frac{5}{32}(am_0) + \ldots. \tag{4.10}$$

From the result in Eq. (4.10), it is clear that d_4 has a simple pole at $am_0 = 0$. Hence, d_4 is divergent in the chiral limit.

Similarly, we can repeat this calculation for all the improvement parameters d_i. We find that each of d_4, d_{EE}, d_{rE}, and d_5 has a simple pole at $am_0 = 0$ and so is divergent in the

chiral limit. Superficially, this behavior appears to violate the first principle of the Fermilab formulation, because it is supposed to work both in the chiral limit and in the heavy quark limit simultaneously. However, we are investigating the discretization effects in the two-quark current matrix elements. We find that, as $a \to 0$ with fixed quark mass ($m_0 \neq 0$), the lattice artifacts vanish, and everything looks regular in this limit. Further progress in this direction will be reported in Ref. [19].

2. Although our results for d_1, d_2, and d_B agree with those in Ref. [9], our result for the improvement parameter d_E differs. Our results for d_E are given in Eq. (3.11), and those in Ref. [9] are

$$d_E(\mathrm{FNAL}) = \frac{1}{2m_b^2} - \frac{\zeta(1+m_0)}{m_b m_0(2+m_0)} + \frac{\zeta(1+m_0)(1-c_E)}{m_0(2+m_0)} \tag{4.11}$$

Hence, the difference is

$$\begin{aligned}\Delta d_E &= d_E(\mathrm{SWME}) - d_E(\mathrm{FNAL}) \\ &= \zeta \frac{-(1+am_0)(2+am_0(2+am_0)) + r_s\zeta am_0(2+am_0) + 2\zeta^2(1+am_0)}{(am_0)^2(2+am_0)^2} \\ &= -\frac{1}{2+am_0} \qquad \text{when we set } \zeta = r_s = 1. \end{aligned} \tag{4.12}$$

It converges to $\left(-\frac{1}{2}\right)$ in the chiral limit and vanishes in the heavy quark limit. The caveats are that $d_E(\mathrm{FNAL})$ is obtained based on NRQCD power counting, for the heavy-heavy meson system, by matching the improved field to the canonical field with a Foldy-Wouthuysen-Tani transformation, while our result $d_E(\mathrm{SWME})$ is derived using a momentum expansion which corresponds to HQET power counting, for the heavy-light meson system. At present, it is not clear how this difference in power counting has a non-trivial effect on Δd_E. We plan to investigate this issue in the near future.

3. Our matching condition yields a unique value for the improvement parameter d_{rE}, even though the action operator corresponding to this parameter is redundant. Since the same isospectral transformations can be applied to the action and the currents [15], a unique value for d_{rE} indicates that the operator basis given in Eq. (2.4) might be incomplete. This issue is under further investigation.

4. It has not been proved yet that the improved quark field is sufficient for the current improvement. The proof can be achieved through the HQET analysis [16, 17, 18] with lattice artifacts incorporated in it. We plan to do this in the near future.

Acknowledgments

We thank Rajan Gupta and Tanmoy Bhattacharya for helpful discussion on V_{cb}. The research of W. Lee is supported by the Creative Research Initiatives Program (No. 20160004939) of the NRF grant funded by the Korean government (MEST). J.A.B. is supported by the Basic Science

Research Program of the National Research Foundation of Korea (NRF) funded by the Ministry of Education (No. 2015024974). W. Lee would like to acknowledge the support from the KISTI supercomputing center through the strategic support program for the supercomputing application research (No. KSC-2014-G3-003). Computations were carried out on the MATHEMATICA workstations at Seoul National University.

References

[1] **BaBar** Collaboration, B. Aubert *et al. Phys. Rev.* **D79** (2009) 012002, [0809.0828].

[2] **BaBar** Collaboration, B. Aubert *et al. Phys. Rev. Lett.* **100** (2008) 231803, [0712.3493].

[3] **BaBar** Collaboration, B. Aubert *et al. Phys. Rev.* **D77** (2008) 032002, [0705.4008].

[4] **Belle** Collaboration, W. Dungel *et al. Phys. Rev.* **D82** (2010) 112007, [1010.5620].

[5] **Fermilab Lattice, MILC** Collaboration, J. A. Bailey *et al. Phys. Rev.* **D89** (2014), no. 11 114504, [1403.0635].

[6] **MILC** Collaboration, J. A. Bailey *et al. Phys. Rev.* **D92** (2015), no. 3 034506, [1503.07237].

[7] C. DeTar *PoS* **LeptonPhoton2015** (2016) 023, [1511.06884].

[8] **HPQCD** Collaboration, H. Na, C. M. Bouchard, G. P. Lepage, C. Monahan, and J. Shigemitsu, *$B \to Dl\nu$ form factors at nonzero recoil and extraction of $|V_{cb}|$*, *Phys. Rev.* **D92** (2015), no. 5 054510, [1505.03925]. [Erratum: Phys. Rev.D93,no.11,119906(2016)].

[9] A. X. El-Khadra, A. S. Kronfeld, and P. B. Mackenzie *Phys. Rev.* **D55** (1997) 3933–3957, [hep-lat/9604004].

[10] C. DeTar, A. Kronfeld, and M. Oktay *PoS* **LATTICE2010** (2010) 234, [1011.5189].

[11] J. A. Bailey, Y.-C. Jang, W. Lee, C. DeTar, A. S. Kronfeld, and M. B. Oktay, *Heavy-Meson Spectrum Tests of the Oktay–Kronfeld Action*, *PoS* **LATTICE2014** (2014) 097, [1411.1823].

[12] J. A. Bailey, Y.-C. Jang, W. Lee, C. DeTar, A. S. Kronfeld, and M. B. Oktay, *Update on Heavy-Meson Spectrum Tests of the Oktay–Kronfeld Action*, *PoS* **LATTICE2015** (2016) 099, [1601.04759].

[13] **SWME** Collaboration, J. A. Bailey, Y.-C. Jang, W. Lee, and J. Leem *PoS* **LATTICE2014** (2014) 389, [1411.4227].

[14] A. S. Kronfeld hep-lat/0205021.

[15] M. B. Oktay and A. S. Kronfeld *Phys. Rev.* **D78** (2008) 014504, [0803.0523].

[16] A. S. Kronfeld *Phys.Rev.* **D62** (2000) 014505, [hep-lat/0002008].

[17] J. Harada, S. Hashimoto, K.-I. Ishikawa, A. S. Kronfeld, T. Onogi, and N. Yamada *Phys. Rev.* **D65** (2002) 094513, [hep-lat/0112044]. [Erratum: Phys. Rev.D71,019903(2005)].

[18] J. Harada, S. Hashimoto, A. S. Kronfeld, and T. Onogi *Phys. Rev.* **D65** (2002) 094514, [hep-lat/0112045].

[19] J. A. Bailey, Y.-C. Jang, W. Lee, J. Leem, *et al. in preparation*.